


 Cite this: *RSC Adv.*, 2021, 11, 8782

# Fabrication and characterization of the ternary composite catalyst system of ZnGA/RET/DMC for the terpolymerization of CO<sub>2</sub>, propylene oxide and trimellitic anhydride

 Ningzhang Liu,<sup>abc</sup> Chuanhai Gu,<sup>abc</sup> Qinghe Wang,<sup>e</sup> Linhua Zhu,<sup>id</sup>\*<sup>abc</sup>  
 Huiqiong Yan<sup>\*abc</sup> and Qiang Lin<sup>id</sup>\*<sup>abcd</sup>

To achieve the poly(propylene carbonate trimellitic anhydride) (PPCTMA) with excellent performance, high molecular weight, enhanced yield and good thermal stability, the ternary composite catalyst system of zinc glutarate/rare earth ternary complex/double metal cyanide (ZnGA/RET/DMC) was proposed to perform the terpolymerization of CO<sub>2</sub>, propylene oxide and trimellitic anhydride. Since the crystallinity and surface activity point of Zn–Co DMC could significantly influence the catalytic ability, mechanical ball milling was applied to increase the surface area of the Zn–Co DMC catalyst with better surface activity point. Moreover, the ZnGA/RET/DMC composite catalytic system and polycarbonate products were comparatively evaluated by XRD, SEM, FT-IR, TGA, NMR, XPS and TEM. Experimental results showed that the ZnGA/RET/DMC composite catalyst system displayed outstanding synergistic effect on the terpolymerization of CO<sub>2</sub>, PO and TMA with better selectivity, activity, and higher molecular weight (*M<sub>w</sub>*) tercopolymer than those of the individual catalyst. According to optimum reaction conditions, the *M<sub>w</sub>* of PPCTMA could be up to 8.29 × 10<sup>4</sup> g mol<sup>-1</sup>, and the yield could be up to 66 g<sub>polymer</sub>/g<sub>cat</sub>. The alternating tercopolymer, PPCTMA, showed wonderful thermal stability and high decomposition temperature (TGA<sub>10%</sub> = 313 °C). A possible synergistic catalytic mechanism of the ZnGA/RET/DMC ternary composite catalyst system was also conjectured.

 Received 12th November 2020  
 Accepted 28th January 2021

DOI: 10.1039/d0ra09630j

[rsc.li/rsc-advances](http://rsc.li/rsc-advances)

## 1 Introduction

Carbon dioxide (CO<sub>2</sub>) is an idealized synthetic C1 raw material because it is abundant, cheap, non-poisonous and non-combustible.<sup>1</sup> Currently, as a primary greenhouse gas, the utilization of CO<sub>2</sub> into commercial products has attracted increasing attention,<sup>2–4</sup> because it can be used as a reproducible carbon source for the synthesis of diverse molecules.<sup>5,6</sup> The copolymerization product prepared by CO<sub>2</sub>, propylene oxide (PO) and the third monomer is a common raw material for many important chemical industries.<sup>7</sup> It is notable that polycarbonate, as an important polymerization product, has a high

molecular weight polymer with carbonate groups in the molecular chain, and is also a kind of tough thermoplastic resin. On account of its excellent properties, such as tasteless, odorless, heatproof, hygiene safety, fatigue resistance, insulativity and high impact, polycarbonates exhibit widespread applications in membranes, protective materials, storage medium, electrical appliance industry, building materials industry, packaging field, and medical devices.<sup>8,9</sup>

The synthesis of polycarbonates through the terpolymerizations of CO<sub>2</sub>, epoxides and a third monomer has been achieved using bimetallic complex, rare earth ternary complex and ionic liquid compounds as catalysts under high-pressure conditions. The representative heterogeneous catalyst systems are zinc carboxylate catalyst, bimetallic catalyst, and rare earth composite catalyst,<sup>10</sup> while the typical homogeneous catalyst systems are porphyrin catalyst, binary metal complex, hybrid ligand and metal system.<sup>11–13</sup> Compared with the heterogeneous catalyst systems, the homogeneous catalyst usually displays some shortcomings, including long reaction period and low yield. It is regrettable that the catalyst with both high catalytic activity and high selectivity to achieve an alternating copolymer has not been found yet.

The typical double metal cyanide (DMC) catalyst systems, such as Zn–Fe DMC, Zn–Co DMC, Zn–Ni DMC and Co–Ni DMC,

<sup>a</sup>College of Chemistry and Chemical Engineering, Hainan Normal University, Haikou, Hainan 571158, P. R. China. E-mail: [linqianggroup@163.com](mailto:linqianggroup@163.com); [zhulinhua1981@163.com](mailto:zhulinhua1981@163.com); [yanhqedu@163.com](mailto:yanhqedu@163.com); Tel: +86-898-65889422

<sup>b</sup>Key Laboratory of Pollution Control of Hainan Province, Hainan Normal University, Haikou, Hainan 571158, P. R. China

<sup>c</sup>Key Laboratory of Natural Polymer Functional Material of Haikou City, College of Chemistry and Chemical Engineering, Hainan Normal University, Haikou 571158, Hainan, P. R. China

<sup>d</sup>Key Laboratory of Tropical Medicinal Resource Chemistry of Ministry of Education, Hainan Normal University, Haikou, Hainan 571158, P. R. China

<sup>e</sup>Venturepharm (Hainan) Co., Ltd, Haikou, Hainan 570314, P. R. China



have been researched in the last few decades.<sup>14–16</sup> Especially, Zn–Co DMC was more conducive to promoting the synthesis of high yield and pure color product. In 2004, Chen *et al.*, reported on a double metal cyanide complex based on a  $Zn_3[Co(CN)_6]_2$  catalyst that was prepared in the presence of different organic solvents, and was used in the copolymerization of  $CO_2$  and cyclohexene oxide.<sup>17</sup> The catalysts showed good catalytic activity, and their turnover number and turnover frequency reached up to 3300 and  $1650\text{ h}^{-1}$ . However, the polymerization conditions involved in the catalyst were relatively harsh because the temperature must reach  $95\text{ }^\circ\text{C}$  and the pressure must be over 3.8 MPa. Zhou and co-workers obtained the Zn–Co DMC with higher crystallinity by traditional solvent synthesis method, the molar fraction of  $CO_2$  in the copolymer was over 30% when the copolymerization of epoxides and  $CO_2$  was performed at  $60\text{ }^\circ\text{C}$  for a period of 12 h.<sup>18</sup> Nevertheless, the higher crystallinity and lower surface area and surface activity point resulted in lower catalytic efficiency, restricting the industrial production. Many investigators have paid attention to adding the adjuvant into DMC catalysts to gain a copolymer with better product, but the experimental results were still unsatisfactory. Liu and coworkers successfully synthesized Zn–Co DMC using trimesic acid as an initiation-transfer agent, but the relative molecular weight of the poly(propylene carbonate) (PPC) copolymer was between 1400 and  $3800\text{ g mol}^{-1}$ .<sup>19</sup> The crystallinity and surface area of DMC were discovered to be the decisive factors to restrict the catalytic activity, and the DMC catalyst with much surface activity point remarkably raised the chemical efficiency. In order to obtain a small particle size of bimetallic catalysts, Bian and co-workers used thermally expanded graphite (TEG) as the support of catalysts for the direct synthesis of DMC.<sup>20</sup> The experimental results showed that the prepared Cu–Ni DMC/TEG catalysts displayed excellent catalytic activity and selectivity. However, the better conversion of the reactant could be carried out under the high temperature conditions at  $100\text{ }^\circ\text{C}$ . The improvement of the DMC systems has been become the main path to enhance its catalytic activity to synthesize an alternating copolymer with high yield, high molecular mass, and good thermal stability under the mild reaction conditions, which has not come true so far.

Another typical catalyst for  $CO_2$  and epoxide copolymerization was the ZnGA catalyst. ZnGA easily prepared by the use of zinc oxide and glutaric acid in toluene at high temperature can effectively open the loop on epoxide and promote the combination of  $CO_2$  and epoxide, thus obtaining the polycarbonate with high  $M_w$  and high yield. For example, Duan *et al.* reported that ZnGA synthesized from ZnO and glutaric acid under magnetic stirring at constant temperature conditions could catalyze the  $CO_2$ /PO copolymerization for the synthesis of PPC with high  $M_w$  and broad distributions under different pressures.<sup>21</sup> In recent years, several researchers also paid attention to optimal reaction conditions for modifying the ZnGA catalyst. Wang and co-workers found that ZnGA could be dispersed on the surface of acid-treated montmorillonite (MMT) in quinoline to prepare the ZnGA–MMT catalyst.<sup>22</sup> Although ZnGA–MMT can catalyze the copolymerization of  $CO_2$ /PO to obtain a polycarbonate with high yield and high glass transition temperature for application, the poor thermal stability

of polycarbonate had impeded the industrialization of the ZnGA catalyst.

Rare-earth ternary (RET) ( $Y(CCl_3COO)_3$ –ZnEt<sub>2</sub>–glycerine) catalyst is a typical heterogeneous catalyst, which has shown high catalytic activity to the copolymerization of  $CO_2$  and epoxides. Quan *et al.* achieved the copolymerization of  $CO_2$  and epoxide using rare-earth ternary catalysts under 3.5–4.0 MPa at 65–70  $^\circ\text{C}$ .<sup>23</sup> Although the RET catalysts successfully synthesized the copolymer, it still displayed poor catalytic activity in comparison with ZnGA, and the by-products also emerged in the copolymer.

It is worth noting that the combination of different catalyst systems may be an effective way to facilitate the copolymerization of  $CO_2$  and epoxides. Meng *et al.* applied a combinatorial catalyst of DMC/ZnGA to catalyze the copolymerization of propylene oxide and  $CO_2$ , attaining the PPC with high  $M_w$  and yield whose  $T_g$  was  $42.0\text{ }^\circ\text{C}$ .<sup>24</sup> At the same time, they found a Salen–Co(III)/DMC catalyst system as a highly effective catalyst for  $CO_2$  and cyclohexene oxide copolymerization.<sup>25</sup> This catalyst displayed the best efficiency at a ratio of Salen–Co(III)/DMC = 1 : 3, and the obtained PPC polycarbonate content was more than 90%.

In this work, in order to obtain an efficient catalytic system, thereby synthesizing polycarbonate products with excellent performance, high  $M_w$ , enhanced yield and good thermal stability, the ternary composite catalyst system of ZnGA/RET/DMC was proposed to conduct the terpolymerization of  $CO_2$ , propylene oxide and trimellitic anhydride. This proposal was based on the high catalytic activity of Zn–Co DMC complexes, the high selectivity of ZnGA and the good stability of RET. In view of the crystallinity and surface activity point of Zn–Co DMC, which could significantly influence the catalytic ability, mechanical ball milling was employed during the synthetic process to increase the surface area of the Zn–Co DMC catalyst with a better surface activity point. Additionally, the physical and chemical properties of the ZnGA/RET/DMC composite catalytic system and polycarbonate products were comparatively evaluated by XRD, SEM, FT-IR, TGA, NMR, XPS and TEM. The objective of this study was to explore the synergistic effects of the individual catalyst of ZnGA, RET and DMC, and their possible catalytic mechanism.

## 2 Experimental

### 2.1. Materials

Trimellitic anhydride (97%), potassium hexacyanocobaltate ( $K_3Co(CN)_6$ ) (98%), zinc oxide (99%), *tert*-butyl alcohol ( $\geq 95\%$ ), and zinc chloride ( $\geq 98\%$ ) were employed as obtained. Trichloroacetic acid and glutaric acid were used after drying. Carbon dioxide ( $CO_2$ ) with a purity of 99.999% was directly used. Yttrium oxide, sodium carbonate anhydrous, glycerin, 1,4-dioxane, diethyl zinc solution, methylbenzene, propylene oxide (PO) analytical grade was provided by Aladdin and directly employed in the experiments.

### 2.2. Catalyst synthesis

**2.2.1 Synthesis of Zn–Co DMC.** 6.6 g  $K_3Co(CN)_6$  and 8.18 g  $ZnCl_2$  reactants were put into a ball mill tank and mixed, and



a small amount of *tert*-butanol was added as an auxiliary solution. Several small balls with diameters of 20 mm, 10 mm and 6 mm were put into the ball-milling tank. After completion, the ball-milling tank was put into the ball mill, and the milling time was set. The rotation frequency was initiated to start running, and it was set to stop running after the ball milling proceeded for a certain period of time. The product was then taken out, dissolved in 20 mL of a 1 : 1 solution of *tert*-butanol and deionized water, stirred, washed, and filtered. Finally, the deposit was placed in a vacuum oven at 50 °C to dry for more than 15 h. For comparison, according to the literature, we also used the traditional water bath method to synthesize Zn–Co DMC.

### 2.2.2 Synthesis of the DMC/RET composite catalyst

*Synthetic method of trichloroacetic acid (Y(CCl<sub>3</sub>OO)<sub>3</sub>).* Weigh 0.01 mol Y<sub>2</sub>O<sub>3</sub> in a beaker, add 50 mL of distilled water, ultrasonically disperse for 10 minutes, and then place it on a magnetic stirring table. Add diluted HCl (5 wt%) to the Y<sub>2</sub>O<sub>3</sub> solution to fully react. Add 1 mL HCl every 2 minutes to make the reaction more complete until the reaction solution is clear. Add enough Na<sub>2</sub>CO<sub>3</sub> to the reaction solution to precipitate Y<sup>3+</sup>. Weigh 0.06 mol CCl<sub>3</sub>COOH, add an appropriate amount of distilled water to dissolve, accelerate the dissolution with ultrasound, and pour into the precipitate to fully react the two until the precipitate disappears. After full reaction, it was dried in vacuum at 60 °C for 6 h.

Under the protection of N<sub>2</sub>, add 0.45 g of glycerol to a three-necked flask, add an appropriate amount of Y(CCl<sub>3</sub>OO)<sub>3</sub> and 1,4-dioxane, and react at 60 °C for 1 h until the solution is homogeneous. Then, 9.7 mL of diethyl zinc was slowly added to the three-necked flask and reacted for 1. After 1 h, add an appropriate amount of Zn–Co DMC to the white suspension of the RET complex. After aging at 65 °C for 3 h, the synthesized combined catalyst was used directly in the subsequent reaction.

### 2.2.3 Synthesis of the ZnGA/RET/DMC composite catalyst

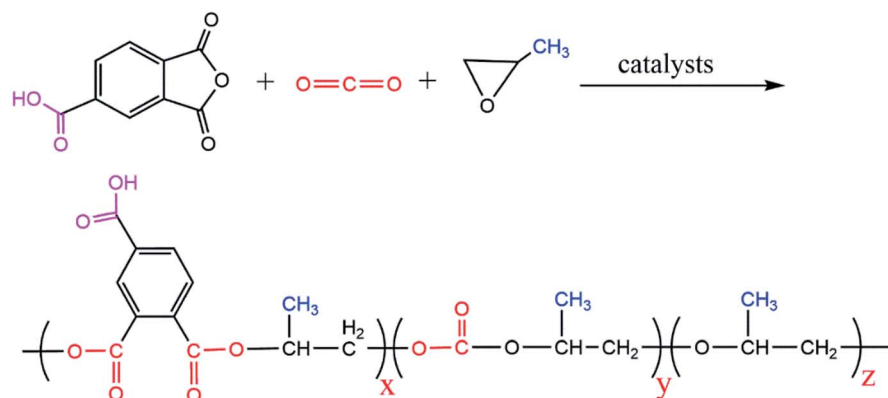
*Synthetic method of ZnGA.* Add 80 mmol zinc oxide and 120 mL toluene into a 250 mL three-necked reaction flask equipped with a stir bar, and slowly add 75 mmol glutaric acid. Start the magnetic stirrer for heating, the reaction temperature is 60 °C, and keep it under vigorous stirring at 850 rpm for 12 h.

After the reaction was completed, it was filtered, and the obtained precipitate was washed with 100 mL of acetone and filtered with suction, which was repeated 3 times in total. The resulting precipitate was dried overnight in a vacuum oven at 55 °C, and the white powder obtained was the ZnGA catalyst.

Under stirring conditions, add the appropriate ZnGA compound and DMC/RET mixture to a 250 mL round bottom flask, and inject 100 mL of toluene. The mixture was slowly heated to 60 °C and vigorously stirred for 24 h. The precipitate was filtered and washed with 100 mL of *t*BuOH and 100 mL of distilled water three times, and the precipitate was separated with a separator. Put the precipitate in a vacuum drying oven at 80 °C for 30 min, then mash the precipitate evenly. Finally, the precipitate was further ground into powder and dried in a vacuum oven at 80 °C for 12 h to obtain a ZnGA/DMC/RET composite catalyst.

### 2.3. Terpolymerization of CO<sub>2</sub>, PO and TMA

The alternating terpolymerization of CO<sub>2</sub>, PO and TMA was executed in a 100 mL stainless steel autoclave equipped with a magnetic suspended vortex type magnetic stirrer and water circulating multi-purpose vacuum pump. The autoclave was washed and heated to 100 °C for 1 hour before use. The composite catalyst and TMA were added in the autoclave, 100 mL of PO was poured and stirred well at the same time. Install the reaction axe and connect the water circulating multi-purpose vacuum pump to start vacuuming. Before the end of the vacuum procedure, another 50 mL of PO was injected into the autoclave through the inlet with a syringe and the inlet was closed quickly. At this point, the feeding process was complete. Then, CO<sub>2</sub> was pumped into the autoclave to make the pressure reach 3 MPa, the autoclave console was opened, the temperature was set at 80 °C and the stirring speed was set to 500 rpm. Then, the polymerization began, CO<sub>2</sub> was continuously injected during the reaction, and ventilation was stopped after the reaction for 15 h. The temperature and agitation were turned off. When the reactor was cooled to room temperature, the remaining CO<sub>2</sub> was released slowly, the autoclave was opened and the products were transferred. 250 mL watery HCl (5 wt%) was added to the products, and it was stirred with a magnetic



Scheme 1 Reaction of CO<sub>2</sub> with PO and TMA.



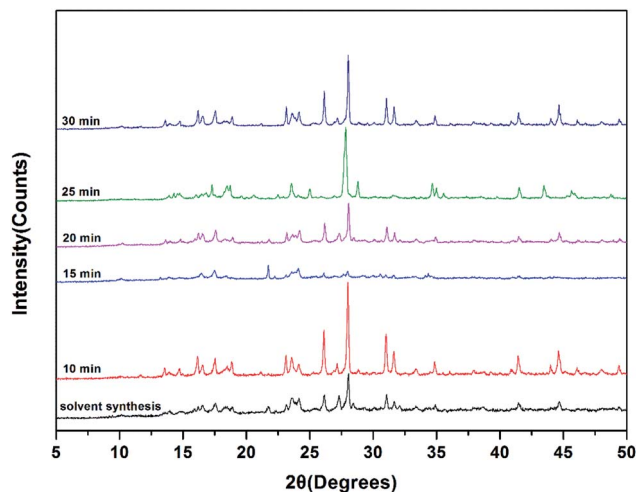


Fig. 1 XRD patterns of the synthesized Zn–Co DMC with different ways.

mixer for 2 h. After stationary layering, discard the upper layer, wash and repeat for 3 times, then add distilled water and stir for 2 h and repeat for 3 times. After the supernatant was poured, it was directly put into the vacuum drying box at 60 °C for 20 h. Vacuum drying proceeded until a constant weight was achieved, and a final weighing and characterization of the product were conducted (Scheme 1).

#### 2.4. Measurements

Scanning electron micrographs (SEM) of the catalyst samples were gathered on JSM-7100F, Nippon Electronics Co. Ltd (JEOL Ltd). A JEM2100 Japanese optical transmission electron microscope was used to observe the morphology of the catalyst, and the acceleration voltage was 200 kV. The X-ray single crystal diffractometer (XRD) with dual light sources was examined by

a Gemini A Ultra from Agilent Technologies, Inc. X-ray photoelectron spectroscopy (XPS) analysis of the catalysts was performed on a Shimadzu KRATOS (Model: Axis Supra, Japan) induced electron emission spectrometer with Al K $\alpha$  (1486.6 eV, 15 mA, 15 kV) X-ray sources. The NMR spectra were achieved by a Bruker AV400 MHz with PAA as the internal standard. Deuteriochloroform (CDCl<sub>3</sub>) was used as a solvent. The FTIR with potassium bromide tablets were examined by a Thermo Fisher Scientific 6700 with spectral resolution of 4 cm<sup>-1</sup> and scanning speed of 10 000 Hz. The molecular mass ( $M_w$ ) of the terpolymers were detected by gel permeation chromatography (GPC) with PL gel of 10  $\mu$ m MIXED-B, 7.5  $\times$  300 mm as the chromatographic column, and using tetrahydrofuran as the eluent and poly-methyl methacrylate as the standard substance. The thermal stabilities of the catalysts and terpolymers were detected with a NETZSCH (Germany), with a temperature range of 30–800 °C at a heating rate of 10 °C min<sup>-1</sup> under a N<sub>2</sub> flowing velocity of 50 mL min<sup>-1</sup>. STA-449F3 thermal gravimetric analyzer from NETZSCH instruments was employed to determine the 10% weight loss rate (TGA<sub>10%</sub>) (30–800 °C, under a N<sub>2</sub> flowing velocity of 50 mL min<sup>-1</sup>).

## 3 Results and discussion

### 3.1. Comparison of Zn–Co DMC catalysts provided with different ways

Because the catalytic activity of Zn–Co DMC is based highly on the active points of the Zn–Co DMC surface area, the catalytic ability is remarkably influenced by the granule size and crystallinity of Zn–Co DMC.<sup>26</sup> The mechanochemical method can effectively reduce the phase purity of the Zn–Co DMC granules and lower the crystallinity. The mechanical ball grinding was adopted into the synthesis of the Zn–Co DMC catalyst, which can enhance the reaction efficiency. XRD patterns of Zn–Co DMC prepared under different ways are shown in Fig. 1. The use

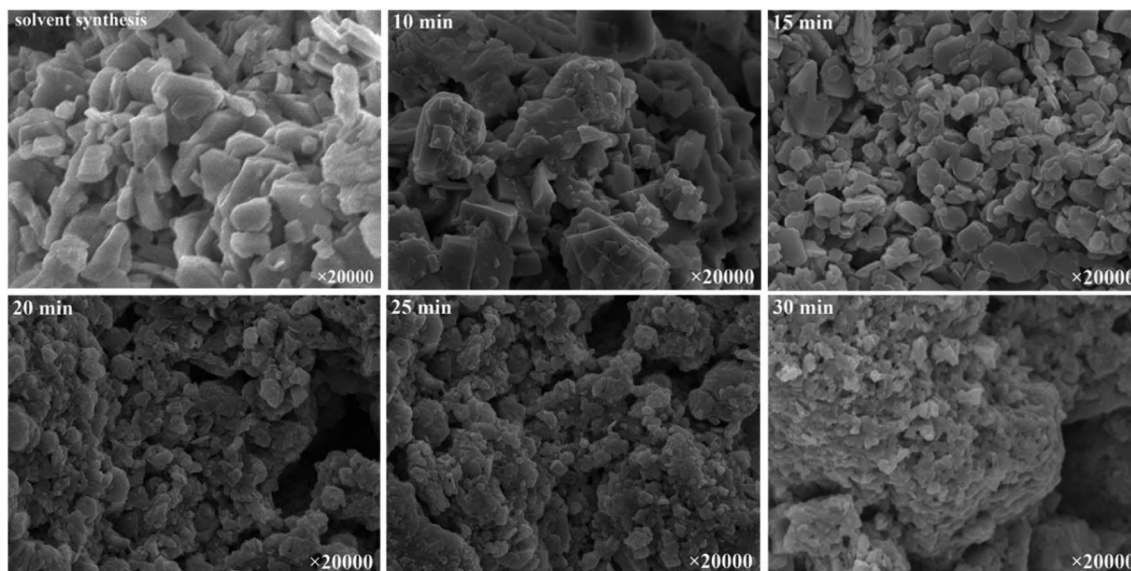


Fig. 2 SEM images of the Zn–Co DMC catalyst samples.



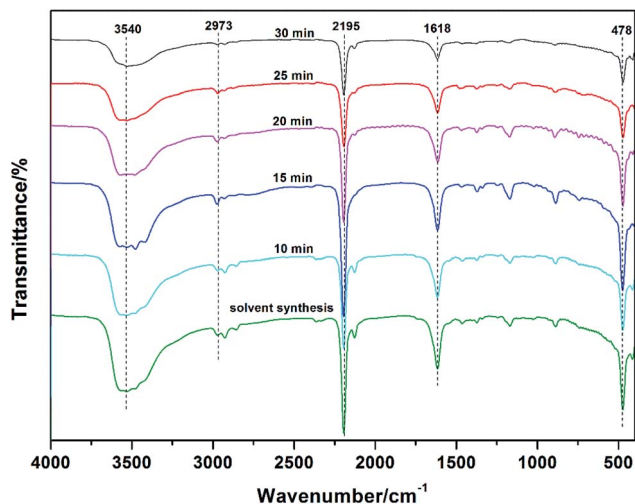


Fig. 3 Comparisons of the FTIR spectra of the Zn-Co DMC samples synthesized for the specified time.

of mechanical ball grinding during the synthesis of the catalyst remarkably lowered the crystallinity of Zn-Co DMC. The XRD patterns of the ball-milled Zn-Co DMC and solvent-based Zn-Co DMC were similar, which proved that the mechanical ball

grinding retained the primitive crystalline structure of Zn-Co DMC. The amorphous of Zn-Co DMC directly resulted in the catalytic ability. The sample milled for 15 min is mainly amorphous according to the obvious lack of sharp lines in the XRD patterns, which indicated that the Zn-Co DMC milled for 15 min displayed the highest catalytic activity. SEM images of Zn-Co DMC prepared under different ways are shown in Fig. 2. The use of mechanical ball grinding during the preparation process dramatically decreased the granule size and crystallinity of Zn-Co DMC. As the exposed active center on the Zn-Co DMC surface area might immediately result in the catalytic effect, the sample that was milled for 15 min was expected to have higher activity than others.

Fig. 3 shows the FTIR spectra of Zn-Co DMC catalysts prepared under different conditions. The C≡N bond stretching vibrational absorption peaks in the Zn<sup>2+</sup>-CN-Co<sup>3+</sup> structural unit of the catalyst all appeared at 2195 cm<sup>-1</sup>. Due to the coordination of Zn<sup>2+</sup> and the C≡N bonds, the C≡N bond in DMC was weakened into a C=N bond. It shows its telescopic vibration absorption peak at 1618 cm<sup>-1</sup>. A small amount of *tert*-butanol was added as the auxiliary liquid during the preparation of the Zn-Co DMC catalyst, so the -OH stretching vibration absorption peak was shown at 3540 cm<sup>-1</sup>. The Co-CN bending vibration absorption peaks appeared at 478 cm<sup>-1</sup>, and the C-H

Table 1 Terpolymerization of CO<sub>2</sub>, PO and TMA over different catalysts<sup>a</sup>

Catalyst	Time (h)	$M_n/M_w$ ( $\times 10^4$ )	Yield <sup>d</sup>	Composition <sup>e</sup> (%)			TGA <sub>10%</sub> /°C
				$f_{CO_2}$	$f_{PO}$	$f_{TMA}$	
DMC (s) <sup>b</sup>	10	1.18/2.35	26.8	10.1	70.6	19.3	186
DMC (10 min) <sup>c</sup>	10	0.88/2.10	24	9.2	67.6	23.2	161
DMC (15 min)	10	2.16/3.67	34	17.2	59.1	23.7	217
DMC (20 min)	10	0.93/2.33	28	10.7	71.4	17.9	183
DMC (25 min)	10	0.81/2.10	24	9.2	67.6	23.2	161
DMC (30 min)	10	0.83/2.08	22	8.8	64.7	26.5	148
RET	20	2.34/6.31	48	22.3	47.2	30.5	285
ZnGA	24	2.61/7.58	58	26.8	42.3	30.9	317
ZnGA/RET/DMC (1 : 1 : 1)	15	2.60/8.03	54	30.2	39.4	30.4	355
ZnGA/RET/DMC (1 : 1 : 10)	15	2.96/8.29	66	34.2	31.4	34.4	393
ZnGA/RET/DMC (1 : 10 : 1)	15	2.70/8.14	62	30.7	35.7	33.6	372

<sup>a</sup> Reaction conditions: CO<sub>2</sub> pressure 3.0 MPa, 80 °C, catalyst addition 0.5 g. <sup>b</sup> DMC was synthesized by solvent synthesis. <sup>c</sup> Means DMC was synthesized by mechanical ball grinding for 10 minutes, and so forth. <sup>d</sup> Yield in g<sub>polym</sub>/g<sub>cat</sub>. <sup>e</sup> Determined by using <sup>1</sup>H NMR spectra.  $f_{CO_2} = (A_{5.28} + A_{4.2}) \times 44 / [(A_{5.28} + A_{4.2}) \times 44 + (A_{5.28} + A_{4.2}) \times 58.08 + A_{3.5} \times 58.08]$ ,  $f_{PO} = (A_{5.28} + A_{4.2}) / [2 \times (A_{5.28} + A_{4.2}) + A_{3.5}]$ ,  $f_{TMA} = 1 - f_{CO_2} - f_{PO}$ .

Table 2 Terpolymerization of CO<sub>2</sub>, PO and TMA over the series of DMC catalysts with different TMA/DMC ratios<sup>a</sup>

DMC <sup>b</sup> (g)	TMA/DMC (g/g)	TOF <sup>c</sup>	$M_w$ ( $\times 10^4$ )	$M_n$ ( $\times 10^4$ )	Yield <sup>d</sup>	TGA <sub>10%</sub> /°C
0.5	19.2	15.05	2.56	1.11	28.6	167
1.0	9.6	11.68	2.02	0.96	25.7	172
1.5	6.4	8.84	1.77	0.93	22.1	162
2.0	4.8	8.5	1.27	0.6	20.4	161
3.0	3.2	6.36	0.93	0.39	17.8	153

<sup>a</sup> Reaction conditions: CO<sub>2</sub> pressure 3.0 MPa, 80 °C and 15 h, catalyst addition 0.5 g. <sup>b</sup> DMC was synthesized by mechanical ball grinding for 15 minutes. <sup>c</sup> TOF in g-polymer/g-Zn h. <sup>d</sup> Yield in g<sub>polym</sub>/g<sub>cat</sub>.



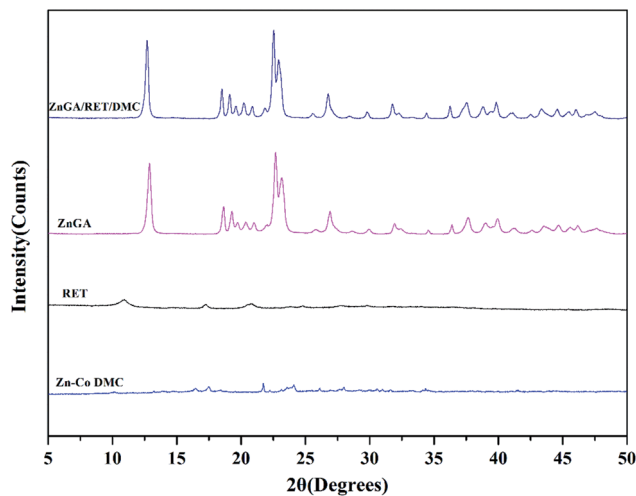


Fig. 4 XRD patterns of the pure DMC, RET, ZnGA and ZnGA/RET/DMC composite catalyst.

vibration absorption peaks appeared at  $2973\text{ cm}^{-1}$ . The chemical shifts of the abovementioned characteristic absorption peaks indicate that mechanical ball milling can effectively promote the *in situ* fusion of the reactants, thereby improving the yield of Zn-Co DMC.

The results of  $\text{CO}_2$ , PO and TMA terpolymerization catalyzed by different catalysts are shown in Table 1. As predicted, the catalyst obtained by ball milling with more surface activity point and lower crystallinity showed significantly higher catalytic activity than that of the catalyst obtained by solvent synthesis. In addition, the catalyst was obtained by ball milling with more surface activity point, resulting in a higher molecular mass of the received PPCTMA. The yield of the PPCTMA growth was

from  $26.8\text{ g}_{\text{polym}}/\text{g}_{\text{cat}}$  to  $30\text{ g}_{\text{polym}}/\text{g}_{\text{cat}}$ , and was followed with an improvement of the molecular mass from  $2.35 \times 10^4\text{ g mol}^{-1}$  to  $2.67 \times 10^4\text{ g mol}^{-1}$ .

For further study of the catalytic behavior of the Zn-Co DMC catalyst in  $\text{CO}_2$ , PO and TMA terpolymerization, the results of the catalyst and the third monomer ratio were researched and are introduced in Table 2. The amount of TMA was kept at 0.05 mol (9.6 g) and that of Zn-Co DMC was grown. The optimum activity was achieved to  $28.6\text{ g}_{\text{polym}}/\text{g}_{\text{cat}}$  at the usage of 0.5 g Zn-Co DMC. Unexpectedly, the molecular weight of the gained PPCTMA had dramatically reduced from  $2.56 \times 10^4\text{ g mol}^{-1}$  to  $0.93 \times 10^4\text{ g mol}^{-1}$  with increasing amount of Zn-Co DMC. These consequences indicated that the increasing amount of Zn-Co DMC catalyst promoted the chain transfer rate rather than the chain propagation rate, leading to the gained terpolymer PPCTMA with lower molecular weight and then poorer thermal stability.

Our comprehension on the Zn-Co DMC catalyzed  $\text{CO}_2$ , PO and TMA terpolymerization was expanded through the assessment of Zn-Co DMC and the characterization of Zn-Co DMC and PPCTMA. These research studies will advance the development of the catalyst for  $\text{CO}_2$ , PO and TMA terpolymerization with high selectivity and high activity to generate carbonate linkages.

### 3.2. Synergistic effect of the ZnGA/RET/DMC composite catalyst

In order to get a catalyst system with high selectivity, high activity and high yield, the ZnGA/RET/DMC composite catalyst was prepared. In this composite catalyst system, the optimum Zn-Co DMC was used as the DMC source.

The impact of the ZnGA/RET/DMC composite catalyst on the terpolymerization of  $\text{CO}_2$ , PO and TMA was researched. The

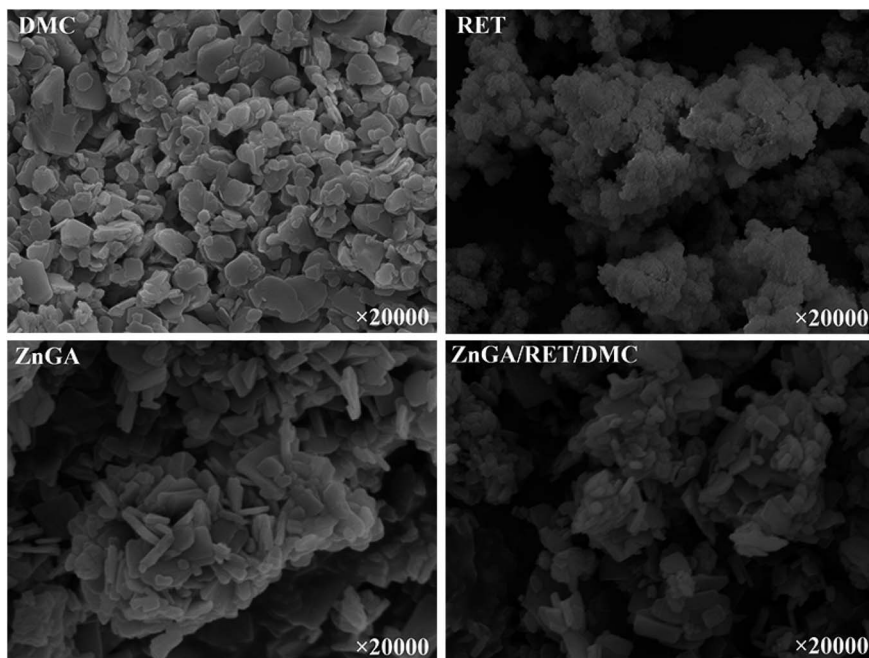


Fig. 5 SEM images of the DMC, RET, ZnGA and ZnGA/RET/DMC composite catalyst samples.



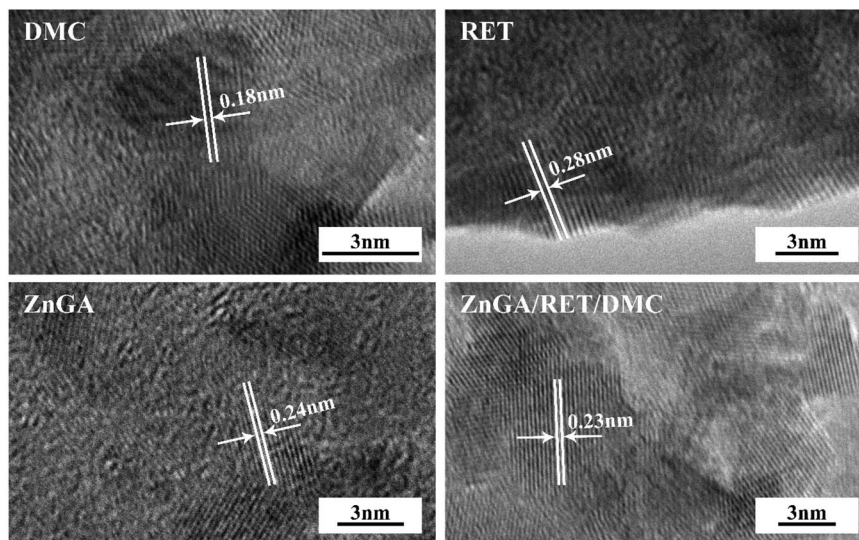


Fig. 6 TEM images of the DMC, RET, ZnGA and ZnGA/RET/DMC composite catalyst samples.

XRD patterns of the DMC, RET, ZnGA, and ZnGA/RET/DMC composite catalyst are displayed in Fig. 4. It clearly showed that the ZnGA/RET/DMC composite catalyst integrated the property of the DMC, RET and ZnGA. For the RET and ZnGA catalyst, three peaks located at around  $2\theta = 10.9, 17.2, 20.8^\circ$  and  $2\theta = 12.9, 22.6, 23.1^\circ$  indicated the gained RET and ZnGA, respectively. The pattern of the ZnGA/RET/DMC composite catalyst included all of the characteristic peaks of Zn–Co DMC with almost exactly the same integral area. The SEM images of the DMC, RET, ZnGA, and ZnGA/RET/DMC composite catalyst are shown in Fig. 5. The pattern of the ZnGA/RET/DMC composite catalyst retained the greater surface activity point and lower crystallinity. The TEM images of the DMC, RET, ZnGA and ZnGA/RET/DMC composite catalyst are shown in Fig. 6. The crystal structure size of all catalysts is less than 1 nanometer. Most of the catalyst is amorphous, which facilitates the

penetration of the reactants and the catalyst, leading to the expansion of the contact surface of the reaction.

The qualitative and quantitative surface formulations of the catalysts were investigated by XPS. The XPS spectra of the catalysts are shown in Fig. 7. The full XPS spectrum of the ZnGA/RET/DMC composite catalyst reveals the co-existence of Zn, Co, O, N, C, Cl and Y in the hybrid structure.

The catalytic effects of the individual RET, ZnGA and DMC in the  $\text{CO}_2$ , PO and TMA terpolymerization are displayed in Table 1. The RET catalyst displayed high yield and high  $M_w$  towards the PPCTMA terpolymer in 20 h, but the reaction time was long. The DMC displayed high catalytic activity towards PPCTMA in 10 h, but the molecular weight and yield of PPCTMA were considerably poor. Meanwhile, the ZnGA displayed high selectivity and high molecular weight towards PPCTMA in 24 h, but the catalytic activity towards PPCTMA was low. By comparing the advantages of the individual RET, ZnGA and DMC catalysts, we looked forward to utilize a ZnGA/RET/DMC composite catalyst into the  $\text{CO}_2$ , PO and TMA terpolymerization to display a synergistic effect cover catalyst with high selectivity, high catalytic activity and high yields.

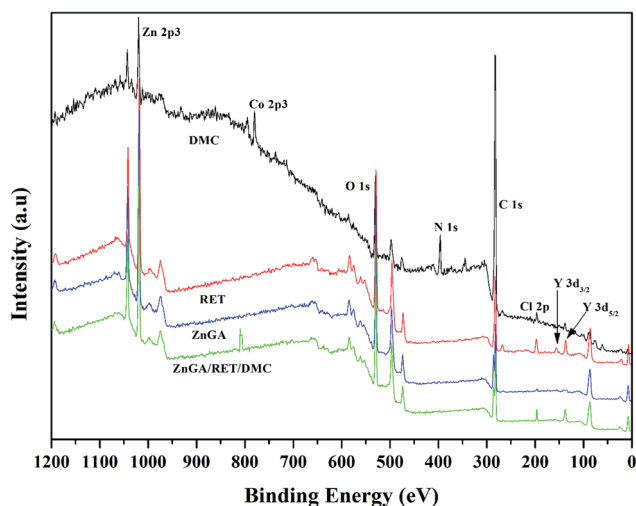


Fig. 7 XPS spectra of various DMC, RET, ZnGA and ZnGA/RET/DMC composite catalysts.

Table 3 Terpolymerization of  $\text{CO}_2$ , PO and TMA catalyzed over the ZnGA/RET/DMC composite catalyst with different reaction times<sup>a</sup>

Time (h)	$M_w (\times 10^4)$	$M_n (\times 10^4)$	Yield <sup>b</sup>	TGA <sub>-10%</sub> /°C
6	1.33	0.74	16	287
9	2.37	1.48	22	291
12	5.61	2.24	48	307
15	8.29	3.07	66	313
18	8.17	3.14	61	302
21	8.31	3.2	59.4	306
24	7.97	2.85	57.4	293

<sup>a</sup> Reaction conditions:  $\text{CO}_2$  pressure: 3.0 MPa, 80 °C, catalyst addition: 0.5 g. <sup>b</sup> Yield in  $\text{g}_{\text{polym}}/\text{g}_{\text{cat}}$ .



Just as we expected, the utilization of the ZnGA/RET/DMC composite catalyst displayed a high catalytic activity in a much lower reaction time compared to that of the RET or ZnGA catalyst. As shown in Table 1, increasing the amount of RET or ZnGA ratio in the ZnGA/RET/DMC composite catalyst only resulted in dramatically improving the molecular weight of PPCTMA, but the others had not changed much. These consequences indicated that the DMC, RET and ZnGA catalyst tended to display specific catalytic characteristic as a composite catalyst system. The yield of the gained PPCTMA was low until it reacted for 9 h (Table 3). From 9 to 12 h, the PPCTMA yield was significantly grown from 22 to 48  $\text{g}_{\text{polym}}/\text{g}_{\text{cat}}$ , indicating that the ZnGA/RET/DMC composite catalyst was in an origination period during the first 9 h. When there was only the DMC catalyst, the terpolymerization course ended in 10 h. These consequences disclosed that RET and ZnGA played a major role in the ZnGA/RET/DMC catalyzed system; they coordinated with the C=O bond of CO<sub>2</sub> and TMA. The highest catalytic activity achieved 66  $\text{g}_{\text{polym}}/\text{g}_{\text{cat}}$  in 15 h. Table 3 also shows that the molecular weight and thermal stability of the terpolymer gained at 15 h maintained the same characteristics as those of the DMC catalyst. The CO<sub>2</sub>, PO and TMA terpolymerization by the ZnGA/RET/DMC composite catalyst displayed high catalytic activity and excellent terpolymerization products, which demonstrated that the ZnGA/RET/DMC composite catalyst displayed a synergistic effect in CO<sub>2</sub>, PO and TMA terpolymerization, while the terpolymerization of CO<sub>2</sub>, PO and TMA catalyzed by the ZnGA/RET/DMC composite catalysts with diverse ZnGA/RET/DMC ratios is displayed in Table 1. Extension of the reaction time to more than 15 h resulted in a dramatic generation of the by-product, for example cyclic carbonate. This would lead to the rapid decrease of the catalytic activity of the ZnGA/RET/DMC composite catalyst to form polycarbonate.<sup>27</sup> Comparing the study, if the DMC, RET and ZnGA catalyst were added synchronously without pre-processing, the catalytic activity, selectivity and molecular weight were much poorer than that of the ZnGA/RET/DMC composite catalyst, indicating no synergistic effect had taken place.

In order to further investigate the role of each individual catalyst in the composite catalyst, one catalyst was reduced during the preparation of the composite catalyst, and the effect of the composite catalyst on the ternary copolymerization of CO<sub>2</sub>, PO and TMA was investigated, as shown in Table 4. The

Table 4 Results of the ternary copolymerization of CO<sub>2</sub>, PO and TMA catalyzed by different composite catalysts<sup>a</sup>

Composite catalyst	Yield <sup>b</sup>	$f_{\text{CO}_2}$ <sup>c</sup> /%	TGA <sub>10%</sub> <sup>c</sup> /°C
ZnGA/RET	23	30.3	274
ZnGA/DMC	57	21.7	270
RET/DMC	52	32.1	182
ZnGA/RET/DMC	66	34.2	313

<sup>a</sup> Reaction conditions: CO<sub>2</sub> pressure: 3.0 MPa, 80 °C and 15 h, catalyst addition: 0.5 g. <sup>b</sup> Yield in  $\text{g}_{\text{polym}}/\text{g}_{\text{cat}}$ . <sup>c</sup> Determined by using <sup>1</sup>H-NMR spectra.  $f_{\text{CO}_2} = (A_{5.28} + A_{4.2}) \times 44 / [(A_{5.28} + A_{4.2}) \times 44 + (A_{5.28} + A_{4.2}) \times 58.08 + A_{3.5} \times 58.08]$ .

ZnGA/RET/DMC composite catalyst catalyzed the terpolymerization of CO<sub>2</sub>, PO and TMA, and the yield was 66  $\text{g}_{\text{polym}}/\text{g}_{\text{cat}}$ .  $f_{\text{CO}_2} = 34.2\%$ , TGA<sub>10%} = 313 °C. When the DMC catalyst is removed, the yield of the product obtained by ZnGA/RET catalysis is relatively low, only 23  $\text{g}_{\text{polym}}/\text{g}_{\text{cat}}$ .  $f_{\text{CO}_2}$  and TGA<sub>10%} did not change significantly. When the RET catalyst was removed, the  $f_{\text{CO}_2}$  of the product obtained by ZnGA/DMC catalysis was only 21.7%, and the yield and TGA<sub>10%} did not change significantly. When the ZnGA catalyst is removed, the thermal stability TGA<sub>10%} of the product obtained by RET/DMC catalysis is only 182 °C, and the yield and  $f_{\text{CO}_2}$  have not changed significantly. The above results indicate that DMC, RET and ZnGA play the role of improving the catalytic activity, selectivity and thermal stability in the ZnGA/RET/DMC composite catalyst, respectively.</sub></sub></sub></sub>

### 3.3. Characteristics of the alternating tercopolymer PPCTMA

The <sup>1</sup>H NMR spectrum in Fig. 8(a) confirmed the formation of PPCTMA. Peaks a, b, c and d were the characteristics of the PPCTMA terpolymer chain. The corresponding characteristic peaks in the spectrum are shown below: <sup>1</sup>H-NMR (CDCl<sub>3</sub>),

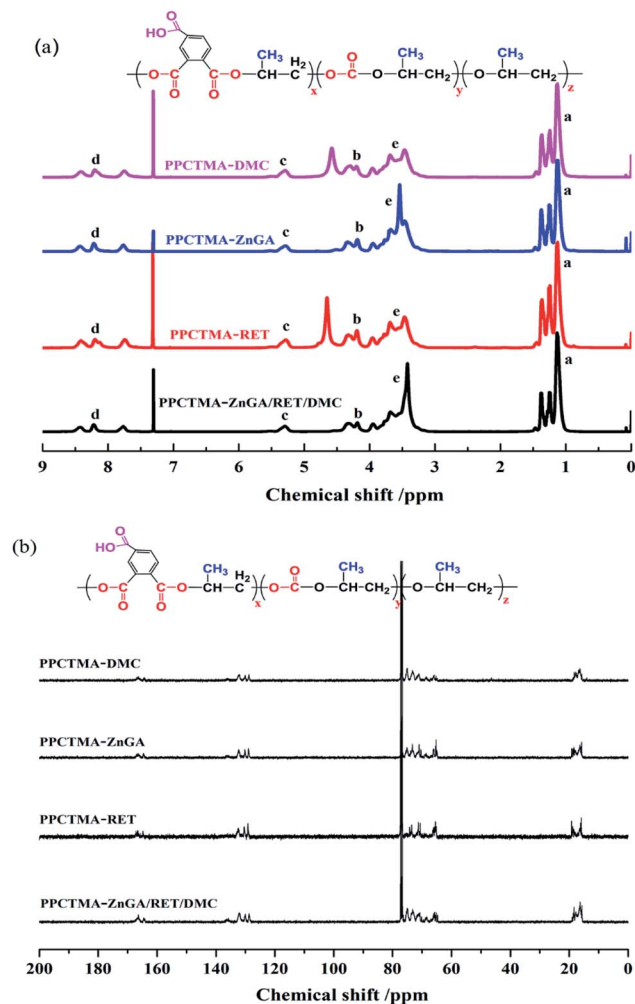


Fig. 8 <sup>1</sup>H and <sup>13</sup>C NMR spectra of the tercopolymer PPCTMA synthesized by using ZnGA/RET/DMC as the catalyst.



$\delta$  (ppm)  $a = 1.25$  ( $\text{CH}_3$ ),  $b = 4.2$  ( $\text{CH}_2(\text{CO}_3)$ ),  $c = 5.28$  ( $\text{CH}(\text{CO}_3)$ ),  $d = 7.76$ – $8.43$  ( $\text{CH}$ ),  $e = 3.45$ – $3.69$  ( $\text{CH}_2\text{CH}$ ). There is no peak at 2.3 ppm, demonstrating that no PO self-reaction was synthesized as the by-product. Simultaneously, the signals did not appear at 4.62 ppm in the  $^1\text{H}$  NMR spectra of PPCTMA, indicating that no cyclic carbonates were formed as by-products. It was likely that the introduction of TMA could inhibit the synthesis of cyclic carbonates. The peaks at 3.68 ppm and 1.45 ppm were assigned to the hydrogens in the ether linkage of propylene oxide. It is deduced that the synthesized PPCTMA tercopolymer displayed an almost exactly alternating molecular structure. Fig. 8(b) shows the  $^{13}\text{C}$  NMR( $\text{CDCl}_3$ ) spectra of PPCTMA. The carbonate chain segment is 164.4–166.3 (OCOO), 64.7–68.3 ( $\text{CH}_2$ ), 73–75 ( $\text{CH}$ ), and 16.3 ( $\text{CH}_3$ ). Polyether chain segment: 73.2 ( $\text{CH}$ ), 68.2 ( $\text{CH}_2$ ), 16.4 ( $\text{CH}_3$ ), and 77.2 as the solvent peak. This further confirmed the presence of polycarbonate in the synthesized polymer.

Fig. 9 displays a typical FTIR spectrum of the gained tercopolymer PPCTMA. The peaks at  $1727\text{ cm}^{-1}$  and  $1240\text{ cm}^{-1}$  were the  $\text{C}=\text{O}$  and  $\text{C}-\text{O}$  bonds of the carbonate group, respectively, and confirmed the internalisation of  $\text{CO}_2$  into the terpolymer chain. The peak at  $1571\text{ cm}^{-1}$  was found to be responsible for the asymmetric stretching vibration of the  $-\text{CO}_2^-$  carboxylate ions, demonstrating the presence of the carboxylate ions in PPCTMA.

As displayed in Table 1, the low molecular weight terpolymer was gained by DMC-catalysed terpolymerization and caused a significantly reduced thermal stability. The activity of the ZnGA and RET catalyst were much lower than that of the DMC catalyst, but they had much higher selectivity and a high molecular weight PPCTMA was gained. When the composite catalyst ZnGA/RET/DMC was used, the molecular weight of the gained tercopolymer PPCTMA was  $8.29 \times 10^4\text{ g mol}^{-1}$  (in Table 1), which maintained the characteristics of the ZnGA and RET catalyst. In addition, the reaction time took longer from 10 to 15 h, which was still much shorter than that of the RET and ZnGA catalytic tercopolymer. The molecular weight of PPCTMA

by the ZnGA/RET/DMC composite catalyst displayed a similar mode with that of ZnGA and RET. These results showed that the small amount of DMC catalyst significantly improved the catalytic activity of the composite catalyst, but the primitive defect of the low molecular weight polymer production was prevented.

The thermal properties of the tercopolymer PPCTMA with diverse molecular weights at varying reaction times are shown in Table 3. Both the  $\text{TGA}_{-10\%}$  and yield of the gained PPCTMA increased with the increase of the molecular weight. In Fig. 10, the gained PPCTMA with a molecular weight of  $>8.2 \times 10^4\text{ g mol}^{-1}$  displays a  $\text{TGA}_{-10\%} >230\text{ }^\circ\text{C}$ . In the DMC-catalyzed system, the molecular weight and  $\text{TGA}_{-10\%}$  of the gained PPCTMA were  $2.67 \times 10^4\text{ g mol}^{-1}$  and  $170\text{ }^\circ\text{C}$ , respectively, which were much poorer than the PPCTMA gained by the ZnGA/RET/DMC composite catalyst. The thermal properties of PPCTMA dramatically depended on the internal structure and molecular weight of the alternating tercopolymer. The consequences showed that the ZnGA/RET/DMC composite catalyst displayed a synergistic effect on the terpolymerization of  $\text{CO}_2$ , PO and TMA. This is due to the PPCTMA properties displaying the property of DMC and ZnGA catalytic behavior, and the PPCTMA yield conforming to the RET catalytic feature.

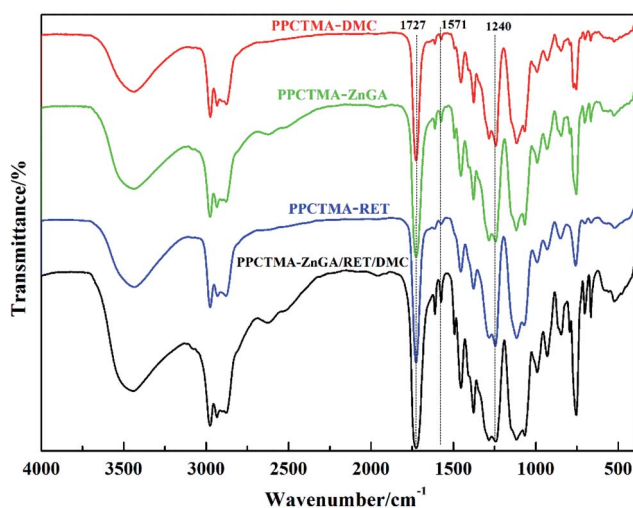


Fig. 9 FTIR spectra of PPCTMA.

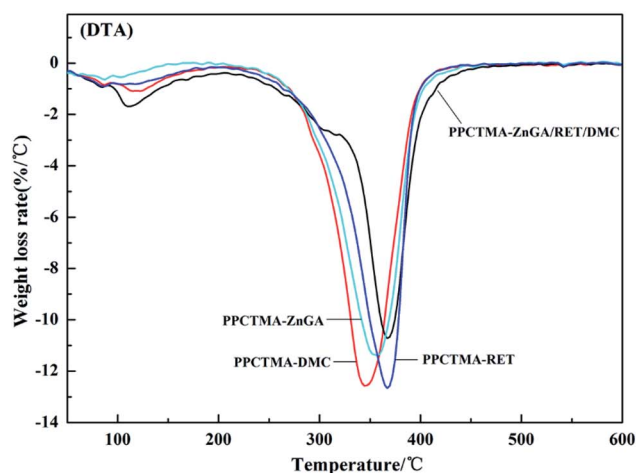
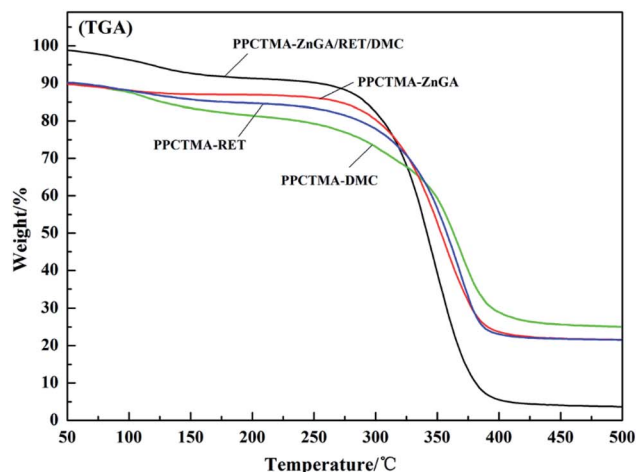
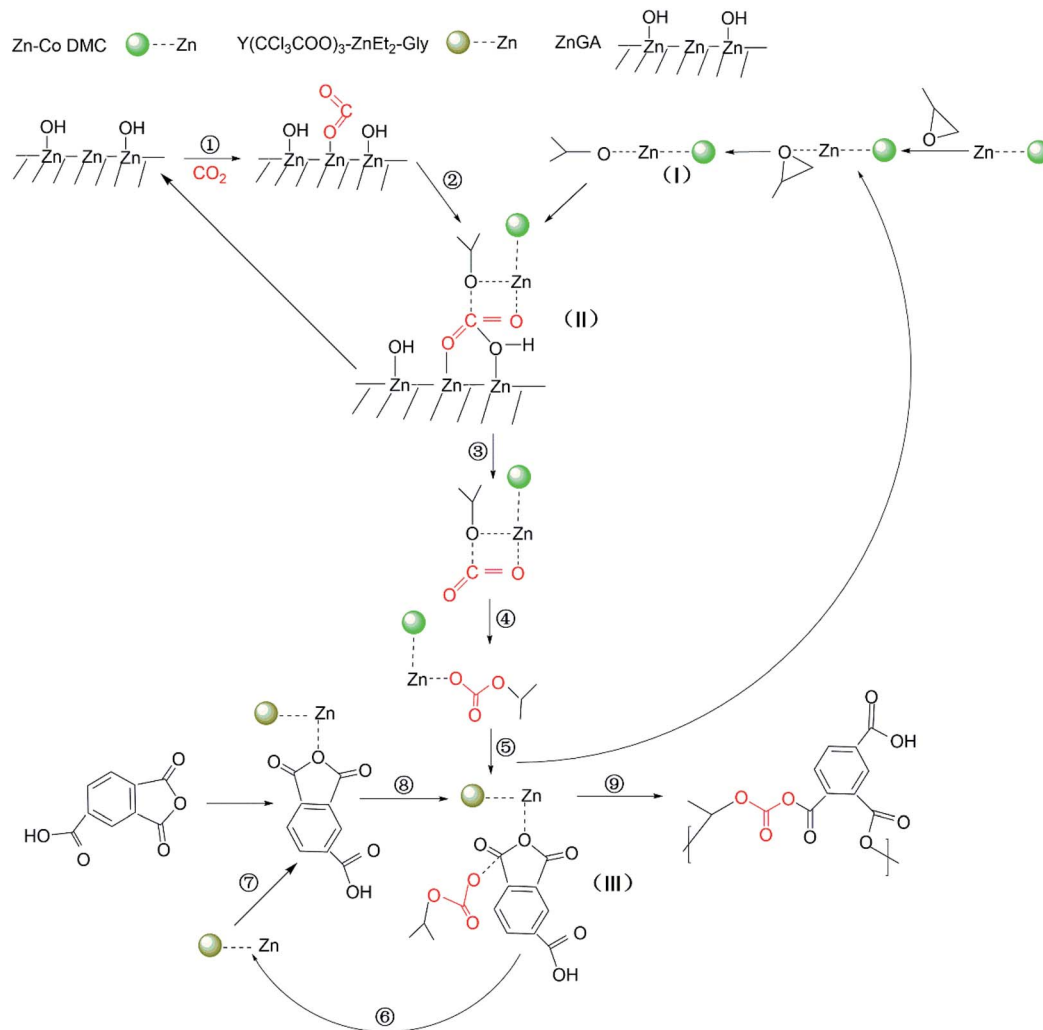


Fig. 10 TGA and DTA curves of the tercopolymer PPCTMA synthesized by the ZnGA/RET/DMC composite catalyst.





Scheme 2 Proposed mechanism of the CO<sub>2</sub>/PO/TMA terpolymerization over the ZnGA/RET/DMC composite catalyst system.

### 3.4. Speculation of the reaction mechanism

According to the previous research studies, it was proved that the terpolymerization of CO<sub>2</sub>, PO and the third monomer originated from the ring-opening polymerization of PO, which was affirmed to be the rate-limiting step of the PO/CO<sub>2</sub>/third monomer terpolymerization. In 2014, Liu *et al.* reported a fundamental of the ZnGA catalyst for the Fineman–Ross plot method, and certificated that the ZnGA catalyst can cause CO<sub>2</sub> reactivity.<sup>28</sup> For the Zn–Co DMC catalyst, Zhang and coworkers thought that the reaction was started with the synergistic action of PO to Zn<sup>2+</sup>, and the succeeding nucleophilic ring-opening of the PO by an –OH group synergistic to the active Zn<sup>2+</sup> center.<sup>29</sup> As for the RET catalyst, Dong *et al.* thought that the copolymerization reaction was initiated by RET, and the catalyst attacked the nucleophile of the intramolecule on the coordinated PO, followed by CO<sub>2</sub> incorporation.<sup>27</sup> As a result, a collaborative mechanism was put forward. In this paper on the synergistic action of the ZnGA/RET/DMC composite catalysts, from the perspective of ligands, it was inferred that Zn–Co DMC has higher activity in the copolymerization of CO<sub>2</sub> and PO.

In the copolymerization reaction of CO<sub>2</sub> and PO, the initial step is the epoxy ring opening. Therefore, Zn–Co DMC preferentially coordinates the ring opening with PO to form intermediate 1. In the reaction system, ZnGA forms [Zn] OH aggregates at the contact interface. The central electron-rich zinc couples with CO<sub>2</sub>, and further coordinates with intermediate 1, breaking the electronic balance in the CO<sub>2</sub> structure to form intermediate 2. The [Zn] OH in the reactant leaves, and CO<sub>2</sub> is successfully coupled with PO to form intermediate 3. After TMA is coordinated with the RET catalyst, it is combined with intermediate 3. The ester bond on one side is opened, and the Zn–Co DMC is finally left to form a polymerized monomer. The above process is repeated to form the CO<sub>2</sub>/PO/TMA terpolymer. According to the terpolymerization results, the mechanism of the CO<sub>2</sub>/PO/TMA terpolymerization catalyzed by ZnGA/RET/DMC composite catalyst system is displayed in Scheme 2.

## 4 Conclusions

Zn–Co DMC with more catalytic activity point and lower crystallinity was obtained by mechanical ball milling. Then, the



ZnGA/RET/DMC composite catalyst was prepared by combining Zn-Co DMC with an appropriate amount of ZnGA and RET. The gained catalysts were employed for the terpolymerization of CO<sub>2</sub>/PO/TMA under suitable reaction conditions. Based on the optimized reaction conditions, the  $M_w$  of the tercopolymer PPC-TMA catalyzed by ZnGA/RET/DMC is  $8.29 \times 10^4 \text{ g mol}^{-1}$ . Furthermore, the terpolymerization yield is  $66 \text{ g}_{\text{polym}}/\text{g}_{\text{cat}}$ , which displays wonderful synergistic catalysis for the CO<sub>2</sub>/PO/TMA terpolymerization. The thermal properties of PPCTMA confirmed that the synthesized alternating tercopolymer PPCTMA displayed excellent thermal stability of TGA<sub>10%</sub> >230 °C. A speculation of the reaction mechanism was put forward to demonstrate that the ZnGA/RET/DMC composite catalyst system displayed excellent synergistic actions on the CO<sub>2</sub>/PO/TMA terpolymerization.

## Conflicts of interest

There are no conflicts to declare.

## Acknowledgements

Financial support is gratefully acknowledged from Hainan Provincial Natural Science Foundation of China (220CXTD436), and the National Natural Science Foundation of China (No. 51963009, 21766007).

## References

- 1 E. Alper and O. Y. Orhan, *Petroleum*, 2017, **3**, 109–126.
- 2 J. M. Spurgeon and B. Kumar, *Energy Environ. Sci.*, 2018, **11**, 1536–1551.
- 3 D. V. Quang, A. Dindi and M. R. A. Zahra, in *CO<sub>2</sub> Separation, Purification and Conversion to Chemicals and Fuels*, Springer, 2019, pp. 153–184.
- 4 J. van Heek, K. Arning and M. Ziefle, *Energy Policy*, 2017, **105**, 53–66.
- 5 D. Riemer, P. Hirapara and S. Das, *ChemSusChem*, 2016, **9**, 1916–1920.
- 6 F. D. Bobbink, S. Das and P. J. Dyson, *Nat. Protoc.*, 2017, **12**, 417.
- 7 S. Ye, S. Wang, L. Lin, M. Xiao and Y. Meng, *Adv. Ind. Eng. Polym. Res.*, 2019, **2**, 143–160.
- 8 F. W. Shaarani and J. J. Bou, *Sci. Total Environ.*, 2017, **598**, 931–936.
- 9 K. Deng, S. Wang, S. Ren, D. Han, M. Xiao and Y. Meng, *ACS Appl. Mater. Interfaces*, 2016, **8**, 33642–33648.
- 10 M. Sankar, T. G. Ajithkumar, G. Sankar and P. Manikandan, *Catal. Commun.*, 2015, **59**, 201–205.
- 11 M. Ramin, J.-D. Grunwaldt and A. Baiker, *J. Catal.*, 2005, **234**, 256–267.
- 12 M. Cokoja, C. Bruckmeier, B. Rieger, W. A. Herrmann and F. E. Kühn, *Angew. Chem., Int. Ed.*, 2011, **50**, 8510–8537.
- 13 S. Mang, A. I. Cooper, M. E. Colclough, N. Chauhan and A. B. Holmes, *Macromolecules*, 2000, **33**, 303–308.
- 14 E. O. P. B. D. Metal, *Chin. J. Polym. Sci.*, 2002, **20**, 453–459.
- 15 Z. Guo, Q. Lin, L. Zhu, X. Wang, Y. Niu, C. Yu and T. Fang, *Nanosci. Nanotechnol. Lett.*, 2014, **6**, 353–356.
- 16 Z. Guo and Q. Lin, *J. Mol. Catal. A: Chem.*, 2014, **390**, 63–68.
- 17 S. Chen, G. R. Qi, Z. J. Hua and H. Q. Yan, *J. Polym. Sci., Part A: Polym. Chem.*, 2004, **42**, 5284–5291.
- 18 T. Zhou, Z. Zou, J. Gan, L. Chen and M. Zhang, *J. Polym. Res.*, 2011, **18**, 2071–2076.
- 19 S. Liu, Y. Qin, X. Chen, X. Wang and F. Wang, *Polym. Chem.*, 2014, **5**, 6171–6179.
- 20 J. Bian, M. Xiao, S. Wang, Y. Lu and Y. Meng, *J. Colloid Interface Sci.*, 2009, **334**, 50–57.
- 21 D. Jintang, W. Jiajun, F. Lianfang, W. Long and G. Xueping, *J. Appl. Polym. Sci.*, 2010, **118**, 366–371.
- 22 J. Wang, Q. Zhu, X. Lu and Y. Meng, *Eur. Polym. J.*, 2005, **41**, 1108–1114.
- 23 Z. Quan, J. Min, Q. Zhou, D. Xie, J. Liu, X. Wang, X. Zhao and F. Wang, in *Macromolecular Symposia*, Wiley Online Library, 2003, vol. 195, pp. 281–286.
- 24 Q. Meng, R. Cheng, J. Li, T. Wang and B. Liu, *J. CO<sub>2</sub> Util.*, 2016, **16**, 86–96.
- 25 Q. Y. Meng, K. Pepper, R. H. Cheng, S. M. Howdle and B. P. Liu, *J. Polym. Sci., Part A: Polym. Chem.*, 2016, **54**, 2785–2793.
- 26 W. Zhang, Q. Lin, Y. Cheng, L. Lu, B. Lin, L. Pan and N. Xu, *J. Appl. Polym. Sci.*, 2012, **123**, 977–985.
- 27 Y. Dong, X. Wang, X. Zhao and F. Wang, *J. Polym. Sci., Part A: Polym. Chem.*, 2012, **50**, 362–370.
- 28 Y. Liu, M. Xiao, S. Wang, L. Xia, D. Hang, G. Cui and Y. Meng, *RSC Adv.*, 2014, **4**, 9503–9508.
- 29 M. Zhang, Y. Yang and L. Chen, *Chin. J. Catal.*, 2015, **36**, 1304–1311.

